Formation control of multiple Euler-Lagrange systems via null-space-based behavioral control

Jie CHEN[1], Minggang GAN[1*], Jie HUANG[2*], Lihua DOU[1] & Hao FANG[1]

[1]*School of Automation, Beijing Institute of Technology, Beijing* 100081*, China;*
[2]*Faculty of Mathematics and Natural Sciences, University of Groningen, Groningen* 9747 AG*, The Netherlands*

Abstract   This paper addresses the formation control problem of multiple Euler-Lagrange systems with model uncertainties in the environment containing obstacles. Utilizing the null-space-based (NSB) behavioral control architecture, the proposed problem can be decomposed into elementary missions (behaviors) with different priorities and implemented by each individual system. A class of novel coordination control algorithms is constructed and utilized to achieve accurate formation task while avoiding obstacles and guaranteeing the model uncertainty rejection objective. By using sliding mode control and Lyapunov theory, the formation performance in closed-loop multi-agent systems is proven achievable if the state-dependent gain of the obstacle avoidance mission is appropriately designed. Finally, simulation examples demonstrate the effectiveness of the algorithms.

Keywords   formation control, obstacle avoidance, Euler-Lagrange system, model uncertainty, behavioral control

1   Introduction

In recent decades, research on coordination control of multi-agent systems has long been of interest owing to its broad applications in many research directions, such as coverage control, consensus, formation control, and flocking [1–3]. The study of Lagrangian systems has attracted the attention of many scholars because of its generic representation of many mechanical systems (e.g., attitude dynamics of rigid bodies, robot manipulators, autonomous vehicles, walking robots) [4–10]. However, most of the existing results can only be applied in ideal environments, and may lose their advantages in complex environments, such as environments with obstacles. Furthermore, the high cost of some actual applications increasingly necessitates high-precision control requirements. Thus, research on high-precision control algorithms in complex environments has many practical implications. This paper focuses on the accurate formation control of multiple Euler-Lagrange systems with model uncertainties in environments containing obstacles.

Applications of robotic system include service, industrial, military, and other civil fields and involve missions like exploration, clean, transportation and manipulation [1,10]. In recent years, control of multi-robot systems and multi-agent systems has received increasing attention as these systems overcome the

---

* Corresponding author (email: agan@bit.edu.cn, autohuangjie@gmail.com)

main dilemmas that an individual robot system is unable to deal with. Essentially, multi-robot systems can increase the overall system effectiveness, by achieving cooperative group performance, which results in lower operational costs, fewer system requirements, higher robustness, stronger adaptivity, and flexible scalability. System's robustness increases through not only unit redundancy but also the simple design of the individual system. The computational load associated with simulation, analysis and control system design is decreasing. Additionally, a simplified model leads to a simplified control system structure. Owing to the aforementioned motivations, three approaches are adopted for controlling multi-robot systems: a centralized approach, a decentralized approach, and a distributed approach [11–18].

Among the plentiful control frameworks for multi-robot systems coordination, behavioral based approaches were previously investigated [19–22], namely the null-space-based behavioral (NSB) control. The NSB architecture differs from single robot control approaches in that, in the behavioral coordination method, it determines a set of suitably defined elementary missions (behaviors) and their priorities. The final behavior is composed by the outputs of the single elementary behaviors. It is noteworthy that the priorities are determined by the mission requirements (or importances) and environmental constraints. In particular, it uses a geometric, hierarchy-based composition of the missions' outputs to obtain the motion reference commands for the robot systems; this composition allows the overall systems to exhibit robustness with respect to eventually conflicting control missions. However, the existing literature mainly connects with asymptotic stability results and usually neglects the influence of model uncertainty and external disturbance. Hence, new results with respect to the finite-time stability would be more valuable to complement its excellent properties of fast convergence rate and high precision.

Currently, with respect to multi-robot systems, several kinds of models are often considered. First, most existing literature studied the first- and second-order systems. Recently, many researchers have begun to focus on the coordination of higher-order multi-agent systems [23], nonlinear dynamics with uncertainties [24,25], nonholonomic mobile robots [26], and general multiple mechanical (Euler-Lagrange) systems [27]. This was motivated by the fact that the nonlinear dynamics cannot be neglected for many kinds of mechanical systems, such as autonomous unmanned ground/air/underwater vehicles [28–30], robotic manipulators, and rigid bodies. Thus, it is unacceptable to model some practical applications using only single- or double-integrator dynamics. Hence, it is of great significance to study the coordinated control of Euler-Lagrange systems, which can generally describe the dynamics of mechanical systems [31,32]. Since the finite-time control design can provide fast convergence and high-precision performance [33,34], it is more meaningful and challenging for multiple Euler-Lagrange systems.

The main contributions of this paper are: (1) The NSB sketch is extended to the application for more complex dynamics. The proposed algorithms can guarantee that the multiple Euler-Lagrange systems constitute and maintain formation while avoiding obstacles. (2) The NSB control strategy is extended to combine with sliding mode control theory. The convergence of the system errors is proved by rigorous finite-time stability proof and the upper bound of the small convergent regions have been calculated accurately. (3) The proposed algorithm is robust to model uncertainty. Furthermore, it successfully avoids the singular problem, which often occurs in the design of the terminal sliding mode.

2 Preliminaries and problem statement

Consider the general multiple mechanical system which is composed of n individual systems and modeled by the Euler-Lagrange formulation as

$$M_i(q_i)\ddot{q}_i + C_i(q_i, \dot{q}_i)\dot{q}_i + g_i(q_i) = \tau_i, \ i = 1, \ldots, n \tag{1}$$

where $M_i(q_i) \in \mathbb{R}^{p \times p}$ is a symmetric positive definite inertia matrix, $q_i \in \mathbb{R}^p$ is the vector of generalized coordinates, $C_i(q_i, \dot{q}_i)\dot{q}_i \in \mathbb{R}^p$ represents the centrifugal and coriolis forces, $g_i(q_i)$ is the gravitational force, and τ_i is the control force on the ith system.

The fundamental properties with respect to the system of (1) can be summarized as follows [27]:

Property 1 (Boundedness). The inertial matrix $M_i(q_i)$ has a lower and an upper bound. For any jth

system, there exist positive constants $\overline{m}_i$, $\underline{m}_i$, k_{Ci} and k_{g_i} such that $0 < \underline{m}_i I_p \leqslant M_i(q_i) \leqslant \overline{m}_i I_p$, and $\|C_i(x, y)\| \leqslant k_{Ci}\|y\|$ for all vectors $x, y \in \mathbb{R}^p$, and $\|g_i(q_i)\| \leqslant k_{g_i}$.

Property 2 (Skew symmetry). $\dot{M}_i(q_i) - 2C_i(q_i, \dot{q}_i)$ is skew symmetric.

Property 3 (Linearity in the dynamic parameters). Eq. (1) can be written as $M_i(q_i)x + C_i(q_i, \dot{q}_i)y + g_i(q_i) = Y_i(q_i, \dot{q}_i, x, y)\Theta_i$ for all vectors $x, y \in \mathbb{R}^p$, where $Y_i(q_i, \dot{q}_i, x, y)$ is the regressor vector of the generalized coordinates and their higher derivatives and Θ_i is the constant parameter vector associated with the ith system.

The objective of this paper is to design a controller for a group of Euler-Lagrange systems to form a formation while avoiding obstacles.

3 Controller design

Motivated by the NSB concept [20–22], to control the shape of multiple systems, aggregate mission functions should be defined according to the control objective. By managing these mission functions and combining them with proper priorities, it is possible to control the overall systems to perform different kinds of missions. In the paper, the mission functions will be defined as the aggregate functions of the global performance of the system. The group of systems moves while keeping a desired formation, as if all the systems were fixed in point of a single system.

3.1 Formation control without obstacles

First, the formation control problem without obstacles is considered. The formation mission drives the group of dynamics to a predefined formation relative to the barycenter. The mission function is defined as $\rho_\varsigma = [(q_1 - q_b)^{\mathrm{T}}, \ldots, (q_n - q_b)^{\mathrm{T}}]^{\mathrm{T}}$, where $q_b = \frac{1}{n}\sum_{i=1}^{n} q_i$ is the coordinate of the barycenter and $\rho_{\varsigma,r} = [\rho_{\varsigma,r1}, \ldots, \rho_{\varsigma,rn}]^{\mathrm{T}}$ denotes the coordinates of all systems in the desired formation. That is, once the formation is defined, the elements of $\rho_{\varsigma,r}$ represent the coordinates of each vehicle in the barycenter reference frame. The formation mission error is defined as $\tilde{\rho}_\varsigma = \rho_{\varsigma,r} - \rho_\varsigma$. The corresponding Jacobian matrix is defined as $Q_\varsigma = \mathrm{diag}\{A, \ldots, A\} \in \mathbb{R}^{pn \times pn}$, and

$$
A = \begin{bmatrix} a & b & \cdots & b \\ b & a & \cdots & b \\ \vdots & \vdots & \ddots & \vdots \\ b & b & \cdots & a \end{bmatrix} \in \mathbb{R}^{n \times n}, \tag{2}
$$

where $a = 1 - \frac{1}{n}, b = -\frac{1}{n}$. In the case of a fixed desired formation ($\dot{\rho}_{\varsigma,r} = 0$) situation, the output of the formation mission function is $\dot{q}_\varsigma = Q_\varsigma^{\dagger}\Delta_\varsigma\tilde{\rho}_\varsigma$, where $Q_\varsigma^{\dagger}$ is the pseudo inverse matrix of Q_ς. Since Q_ς is symmetric and idempotent, $Q_\varsigma^{\dagger} = Q_\varsigma$. The following desired velocity for the formation mission by generalized coordinates form is defined as

$$
\dot{q}_\varsigma = [\dot{q}_{1,\varsigma}^{\mathrm{T}}, \ldots, \dot{q}_{n,\varsigma}^{\mathrm{T}}]^{\mathrm{T}} = Q_\varsigma^{\dagger}\Delta_\varsigma\tilde{\rho}_\varsigma, \tag{3}
$$

where Δ_ς is a positive definite matrix of gains. If $\tilde{\rho}_{\varsigma,r} = 0$ holds, the fixed desired formation is achieved.

The aggregate desired formation velocity of the n systems can be defined as

$$
\dot{q}_r = \dot{q}_\varsigma, \tag{4}
$$

where $\dot{q}_r = [\dot{q}_{1,r}^{\mathrm{T}}, \ldots, \dot{q}_{n,r}^{\mathrm{T}}]^{\mathrm{T}}$ and $\dot{q}_\varsigma = [\dot{q}_{1,\varsigma}^{\mathrm{T}}, \ldots, \dot{q}_{n,\varsigma}^{\mathrm{T}}]^{\mathrm{T}} \in \mathbb{R}^{pn}$.

Combined with the NSB control scheme, a nonsingular fast terminal sliding mode (NFTSM) is constructed for subsequent design:

$$
\sigma = \dot{\tilde{q}} + c_1\tilde{q} + c_2\beta(\tilde{q}), \tag{5}
$$

where c_1 and c_2 are two positive designed parameters, $\tilde{q} = [\tilde{q}_1^{\mathrm{T}}, \ldots, \tilde{q}_n^{\mathrm{T}}]^{\mathrm{T}} = q - q_r$ is the tracking error of the positions. Additionally, $\dot{\tilde{q}} = [\dot{\tilde{q}}_1^{\mathrm{T}}, \ldots, \dot{\tilde{q}}_n^{\mathrm{T}}]^{\mathrm{T}} = \dot{q} - \dot{q}_r$, $\sigma = [\sigma_1^{\mathrm{T}}, \ldots, \sigma_n^{\mathrm{T}}]^{\mathrm{T}}$, $\sigma_i = [\sigma_{i,1}, \sigma_{i,2}]^{\mathrm{T}}$, $\beta(\tilde{q}) = [\beta_1(\tilde{q}_1)^{\mathrm{T}}, \ldots, \beta_n(\tilde{q}_n)^{\mathrm{T}}]^{\mathrm{T}}$, $\beta_i(\tilde{q}_i) = [\beta_{i,1}(\tilde{q}_{i,1}), \beta_{i,2}(\tilde{q}_{i,2})]^{\mathrm{T}}$ and

$$\beta_{i,j}(\tilde{q}_{i,j}) \triangleq \begin{cases} \tilde{q}_{i,j}^r, & \text{for } \bar{\sigma}_{i,j} = 0 \text{ or } \bar{\sigma}_{i,j} \neq 0, \ |\tilde{q}_{i,j}| > \epsilon, \\ \zeta_1 \tilde{q}_{i,j} + \zeta_2 \mathrm{sig}^2(\tilde{q}_{i,j}), & \text{for } \bar{\sigma}_{i,j} \neq 0, \ |\tilde{q}_{i,j}| \leqslant \epsilon. \end{cases}$$

for $i = 1, \ldots, n$, $j = 1, 2$ and $r = \frac{r_1}{r_2}$, where r_1, r_2 are positive odd integers, $\frac{1}{2} < r < 1$, ϵ is a small positive constant, $\zeta_1 = (2 - r)\epsilon^{r-1}$, $\zeta_2 = (r - 1)\epsilon^{r-2}$, $\mathrm{sig}^\beta(\cdot)$ is defined as $\mathrm{sig}^\beta(\boldsymbol{x}) = |\boldsymbol{x}|^\beta \mathrm{sgn}(\boldsymbol{x})$ for $\beta > 0$ and $\mathrm{sig}^\beta(\boldsymbol{x}) = [\mathrm{sig}^\beta(x_i)]^{\mathrm{T}}$ for $\boldsymbol{x} = [x_1, \ldots, x_n]^{\mathrm{T}} = [x_i]^{\mathrm{T}} \in \mathbb{R}^n$, $i = 1, \ldots, n$, and $\mathrm{sgn}(\cdot)$ is defined as the sign function. For this kind of function, it follows that $\frac{\mathrm{dsig}^\beta(\boldsymbol{x})}{\mathrm{d}\boldsymbol{x}} = \beta |\boldsymbol{x}|^{\beta-1}$, and $\bar{\sigma}_{i,j} = \dot{\tilde{q}}_{i,j} + c_1 \tilde{q}_{i,j} + c_2 \tilde{q}_{i,j}^r$.

The time derivative of $\beta_{i,j}(\tilde{q}_{i,j})$ can be obtained as follows:

$$\dot{\beta}_{i,j}(\dot{\tilde{q}}_{i,j}) \triangleq \begin{cases} r\tilde{q}_{i,j}^{r-1}\dot{\tilde{q}}_{i,j}, & \text{for } \bar{\sigma}_{i,j} = 0 \text{ or } \bar{\sigma}_{i,j} \neq 0, \ |\tilde{q}_{i,j}| > \epsilon, \\ \zeta_1 \dot{\tilde{q}}_{i,j} + 2\zeta_2 |\tilde{q}_{i,j}|\dot{\tilde{q}}_{i,j}, & \text{for } \bar{\sigma}_{i,j} \neq 0, \ |\tilde{q}_{i,j}| \leqslant \epsilon. \end{cases}$$

where $\dot{\beta}(\dot{\tilde{q}}) = [\dot{\beta}_1(\dot{\tilde{q}}_1)^{\mathrm{T}}, \ldots, \dot{\beta}_n(\dot{\tilde{q}}_n)^{\mathrm{T}}]^{\mathrm{T}}$ and $\dot{\beta}_i(\dot{\tilde{q}}_i) = [\dot{\beta}_{i,1}(\dot{\tilde{q}}_{i,1}), \dot{\beta}_{i,2}(\dot{\tilde{q}}_{i,2})]^{\mathrm{T}}$. Denote $\dot{q}_\nu = [\dot{q}_{\nu,1}^{\mathrm{T}}, \ldots, \dot{q}_{\nu,n}^{\mathrm{T}}]^{\mathrm{T}} = \dot{q}_r - c_1 \tilde{q} - c_2 \beta(\tilde{q})$ and $\ddot{q}_\nu = [\ddot{q}_{\nu,1}^{\mathrm{T}}, \ldots, \ddot{q}_{\nu,n}^{\mathrm{T}}]^{\mathrm{T}} = \ddot{q}_r - c_1 \dot{\tilde{q}} - c_2 \dot{\beta}(\dot{\tilde{q}})$, then Eq. (5) becomes $\sigma = \dot{q} - \dot{q}_\nu$.

Based on the aforementioned design, we proposed the following adaptive control laws:

$$\tau_i = -C_{\sigma i}\sigma_i - C_{si}\sigma_i^s + Y_i(q_i, \dot{q}_i, \dot{q}_{\nu,i}, \ddot{q}_{\nu,i})\hat{\Theta}_i, \tag{6}$$

$$\dot{\hat{\Theta}}_i = -\Gamma_i^{-1} Y_i(q_i, \dot{q}_i, \dot{q}_{\nu,i}, \ddot{q}_{\nu,i})\sigma_i - \gamma_i \hat{\Theta}_i, \tag{7}$$

where $s = \frac{s_1}{s_2}$, s_1 and s_2 are positive odd integers, and $0 < s < 1$. Furthermore, Y_i is a known regressor matrix, $\hat{\Theta}_i$ is the estimation of Θ_i, and $\tilde{\Theta}_i = \Theta_i - \hat{\Theta}_i$ denotes the estimate error. Additionally, $C_{\sigma i} = c_{\sigma i}I$ and $C_{si} = c_{si}I$ are positive definite and constant matrices. Γ_i is a positive definite matrix, and $\gamma_i > 0$ is a positive design parameter.

Theorem 1. Using the proposed control algorithm (6) and (7) with the desired velocity (4) for the system (1), the generalized system errors $\tilde{q}_{i,j}$ and $\dot{\tilde{q}}_{i,j}$ will converge into the regions $|\tilde{q}_{i,j}| \leqslant \eta_1$ and $|\dot{\tilde{q}}_{i,j}| \leqslant \eta_2$, respectively, in finite time, respectively, where $\eta_1 = \max\{\epsilon, \min\{\frac{|o|}{c_1}, (\frac{|o|}{c_2})^{1/r}\}\}$, $\eta_2 = |o| + c_1\eta_1 + c_2\eta_1^r$.

Proof. Substituting (6) into (1), we get:

$$K_{\sigma i}\sigma_i + K_{si}\sigma_i^s = -M_i(q_i)\dot{\sigma}_i - C_i(q_i, \dot{q}_i)\sigma_i - Y_i(q_i, \dot{q}_i, \dot{q}_{\nu,i}, \ddot{q}_{\nu,i})\tilde{\Theta}_i. \tag{8}$$

Consider the Lyapunov function candidate V_1 as

$$V_1 = V_{\sigma 1} + V_{\rho 1}, \tag{9}$$

where $V_{\sigma 1}$ is considered to prove the stability of the system under the proposed control laws, and $V_{\rho 1}$ is constructed to testify the stability of the formation mission.

$$V_{\sigma 1} = \sum_{i=1}^n \frac{1}{2}\sigma_i^{\mathrm{T}} M_i(q_i)\sigma_i + \sum_{i=1}^n \frac{1}{2}\tilde{\Theta}_i^{\mathrm{T}}\Gamma_i\tilde{\Theta}_i. \tag{10}$$

Taking the derivative of $V_{\sigma 1}$ along with the trajectory of (8), yields:

$$\dot{V}_{\sigma 1} = \sum_{i=1}^n \sigma_i^{\mathrm{T}} M_i(q_i)\dot{\sigma}_i + \sum_{i=1}^n \frac{1}{2}\sigma_i^{\mathrm{T}}\dot{M}_i(q_i)\sigma_i + \sum_{i=1}^n \tilde{\Theta}_i^{\mathrm{T}}\Gamma_i\dot{\tilde{\Theta}}_i$$

$$= -\sum_{i=1}^n \sigma_i^{\mathrm{T}} \left(-\tau_i^d + C_{\sigma i}\sigma_i + C_{si}\sigma_i^s + Y_i(q_i, \dot{q}_i, \dot{q}_{\nu,i}, \ddot{q}_{\nu,i})\tilde{\Theta}_i \right)$$

$$+ \sum_{i=1}^n \gamma_i \tilde{\Theta}_i^{\mathrm{T}}\Gamma_i\hat{\Theta}_i + \sum_{i=1}^n \tilde{\Theta}_i^{\mathrm{T}} Y_i(q_i, \dot{q}_i, \dot{q}_{\nu,i}, \ddot{q}_{\nu,i})\sigma_i$$

$$
\leqslant -\sum_{i=1}^{n} \sigma_i^{\mathrm{T}} C_{\sigma i} \sigma_i - \sum_{i=1}^{n} \sigma_i^{\mathrm{T}} C_{si} \sigma_i^s + \sum_{i=1}^{n} \gamma_i \tilde{\Theta}_i^{\mathrm{T}} \Gamma_i \hat{\Theta}_i
$$

$$
\leqslant -\sum_{i=1}^{n} \sigma_i^{\mathrm{T}} C_{\sigma i} \sigma_i - \sum_{i=1}^{n} \sigma_i^{\mathrm{T}} C_{si} \sigma_i^s - \sum_{i=1}^{n} \frac{\gamma_i \Delta_{\min}(\Gamma_i)}{2} \|\tilde{\Theta}_i\|^2 + \sum_{i=1}^{n} \frac{\gamma_i \Delta_{\min}(\Gamma_i)}{2} \|\Theta_i\|^2,
$$

where Properties 1–3 of (1) are used in the above inequation. With the aid of Lemma 2 from Zhou and Xia [35], we can obtain $\dot{V}_{\sigma 1} \leqslant -\lambda_1 V_{\sigma 1} + \lambda_2$ where $\lambda_1 = \min\{\frac{2k_{\sigma i}}{\Delta_{\max}(M_i(q_i))}, \frac{\gamma_i \Delta_{\min}(\Gamma_i)}{\Delta_{\max}(\Gamma_i)}\}$, $\lambda_2 = \sum_{i=1}^{n} \frac{\gamma_i \Delta_{\min}(\Gamma_i)}{2} \|\Theta_i\|^2$, where $\Delta_{\min}(\cdot)$ and $\Delta_{\max}(\cdot)$ denote the minimum and maximum eigenvalue of Γ_i, respectively. Multiplying both sides of $\dot{V}_{\sigma 1} \leqslant -\lambda_1 V_{\sigma 1} + \lambda_2$ by $e^{\lambda_1 t}$, it can be expressed as $\frac{d}{dt}(V_{\sigma 1}(t) e^{\lambda_1 t}) \leqslant \lambda_2 e^{\lambda_1 t}$. Then, integrating it over the range $[0, t]$, we have $0 \leqslant V_{\sigma 1}(t) \leqslant \frac{\lambda_2}{\lambda_1} + [V_{\sigma 1}(0) - \frac{\lambda_2}{\lambda_1}] e^{-\lambda_1 t}$. Since $0 \leqslant e^{-\lambda_1 t} \leqslant 1$ and $\frac{\lambda_2}{\lambda_1} e^{-\lambda_1 t} > 0$, we can obtain $[V_{\sigma 1}(0) - \frac{\lambda_2}{\lambda_1}] e^{-\lambda_1 t} \leqslant V_{\sigma 1}(0)$. Thus, it yields $0 \leqslant V_{\sigma 1}(t) \leqslant \frac{\lambda_2}{\lambda_1} + V_{\sigma 1}(0)$. Therefore, the boundedness of $\sigma_i, \tilde{\Theta}_i$ is proved, moreover, the boundedness of $\tilde{q}_i$ and $\dot{\tilde{q}}_i$ can be obtained; thus, q_i and $\dot{q}_i$ are bounded for the bounded $q_{r,i}$ and $\dot{q}_{r,i}$. Without loss of generality, we assume that $\|\tilde{\Theta}_i\| \leqslant \varepsilon_i$ with $\varepsilon_i > 0$.

From Property 1 of system (1), it can be easily derived that if q_i, $\dot{q}_i$, $q_{r,i}$, and $\dot{q}_{r,i}$ are bounded, $Y_i(q_i, \dot{q}_i, \dot{q}_{\nu,i}, \ddot{q}_{\nu,i})$ is bounded. Assume that $\|Y_i(q_i, \dot{q}_i, \dot{q}_{\nu,i}, \ddot{q}_{\nu,i})\| \leqslant \varrho_i$. Define $V'_{\sigma 1} = \sum_{i=1}^{n} \frac{1}{2} \sigma_i^{\mathrm{T}} M_i(q_i) \sigma_i$ and take its derivative:

$$
\dot{V}'_{\sigma 1} = -\sum_{i=1}^{n} \sigma_i^{\mathrm{T}} \left(Y_i(q_i, \dot{q}_i, \dot{q}_{\nu,i}, \ddot{q}_{\nu,i}) \tilde{\Theta}_i + C_{\sigma i} \sigma_i + C_{si} \sigma_i^s \right)
$$

$$
\leqslant -\sum_{i=1}^{n} \sigma_i^{\mathrm{T}} C_{\sigma i} \sigma_i - \sum_{i=1}^{n} \sigma_i^{\mathrm{T}} C_{si} \sigma_i^s + \sum_{i=1}^{n} \lambda_3 \|\sigma_i\|_1, \tag{11}
$$

where $\lambda_3 = \max\{\varrho_i \varepsilon_i\}$. With the aid of Lemma 2 [35], Eq. (11) can be rewritten as

$$
\dot{V}_{\sigma 1} \leqslant -\frac{2\Delta_\sigma}{\overline{m}} V_{\sigma 1} - \Delta_s \left(\frac{2}{\overline{m}}\right)^{\frac{1+s}{2}} V_{\sigma 1}^{\frac{1+s}{2}} + \sum_{i=1}^{n} \lambda_3 \|\sigma_i\|_1,
$$

where

$$
\Delta_\sigma = \min\{c_{\sigma 1}, \ldots, c_{\sigma n}\}, \quad \Delta_s = \min\{c_{s1}, \ldots, c_{sn}\},
$$
$$
\overline{m} = \max\{\overline{m}_1, \ldots, \overline{m}_n\}, \quad \underline{m} = \min\{\underline{m}_1, \ldots, \underline{m}_n\}.
$$

Moreover, we obtain $\dot{V}_{\sigma 1} + \mu_1 V_{\sigma 1} + \mu_2 V_{\sigma 1}^{\frac{1+s}{2}} \leqslant 0$ for $\|\sigma\|_1 > o$, where $\mu_1 = \frac{2\Delta_\sigma}{\overline{m}}$, $\mu_2 = \Delta_s(\frac{2}{\overline{m}})^{\frac{1+s}{2}}$, and $o := \min\{\frac{2\lambda_3 \overline{m}}{\underline{m}\Delta_\sigma}, \sqrt[s]{\frac{\lambda_3}{\Delta_s}(\frac{\overline{m}}{\underline{m}})^{\frac{1+s}{2}}}\}$ is a small region, and we can minimize the small region by choosing large control gains. Thus, the finite-time convergence of σ is proved and $\|\sigma\|_1 \leqslant o$ in finite time according to the definition of finite-time stability from Yu et al. [36]. Furthermore, we get that $\tilde{q}_{i,j}$ and $\dot{\tilde{q}}_{i,j}$ will converge to η_1 and η_2, respectively, in finite time, where $\eta_1 = \max\{\epsilon, \min\{\frac{|o|}{c_1}, (\frac{|o|}{c_2})^{1/r}\}\}$, and $\eta_2 = |o| + c_1 \eta_1 + c_2 \eta_1^r$.

Second, the stability of the formation mission should be proved. Define the Lypunove function candidate $V_{\rho 1}$ for the formation mission as

$$
V_{\rho 1} = \frac{1}{2} \tilde{\rho}_\varsigma^{\mathrm{T}} \gamma_\varsigma \tilde{\rho}_\varsigma, \tag{12}
$$

where γ_ς is parameter to be designed. Using the fact that $\dot{\rho}_\varsigma = Q_\varsigma \dot{q}_\varsigma$, $\dot{q}_\varsigma = Q_\varsigma^\dagger \Delta_\varsigma \tilde{\rho}_\varsigma$ and $Q_\varsigma Q_\varsigma^\dagger = I_{np}$, we can obtain the derivative of (12) as $\dot{V}_{\rho 1} = -\tilde{\rho}_\varsigma^{\mathrm{T}} \gamma_\varsigma Q_\varsigma Q_\varsigma^\dagger \Delta_\varsigma \tilde{\rho}_\varsigma \leqslant 0$. It can be seen that the formation always maintains stable, and the tracking errors $\tilde{q}_{i,j}$ and $\dot{\tilde{q}}_{i,j}$ will converge to η_1 and η_2, respectively, in finite time.

3.2 Formation control with obstacles

Unlike traditional formation and obstacle avoidance methods [37–41], this section is based on the NSB scheme. The NSB statically determines a set of suitably defined elementary missions with different priorities.
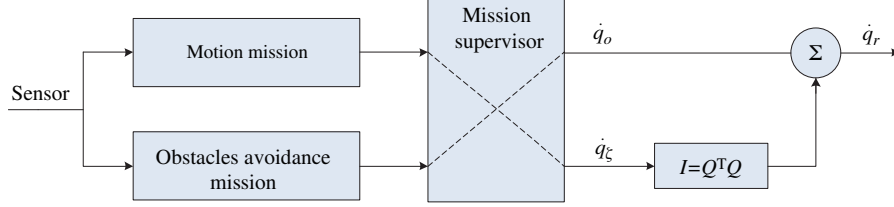
Figure 1 Sketch of the NSB with 2-missions. The mission supervisor is in charge of changing the relative priorities among the missions.

In order to control a platoon of systems to form a formation and avoid obstacles in finite time, the two mission functions, motion mission and obstacle avoidance mission, should be considered simultaneously. The priority of motion is lower than that of obstacle avoidance. The overall mission achievement is obtained by properly combining the two missions with the aid of the null-space projection mechanism [22] which is shown in Figure 1. Hence, the desired velocity is given by

$$\dot{q}_r = \dot{q}_o + (I - Q_o^\dagger Q_o)\dot{q}_\varsigma, \tag{13}$$

where $\dot{q}_r = [\dot{q}_{1,r}^{\rm T}, \ldots, \dot{q}_{n,r}^{\rm T}]^{\rm T}$, and $\dot{q}_o = [\dot{q}_{1,o}^{\rm T}, \ldots, \dot{q}_{n,o}^{\rm T}]^{\rm T} \in \mathbb{R}^{pn}$ is the desired velocity for obstacle avoidance mission, $\dot{q}_{i,o} = Q_{i,o}^\dagger \Delta_{i,o}\tilde{\rho}_{i,o} = (\max\{d_i - \|q_i - q_{i,o}\|, 0\} + \|\dot{q}_i - \dot{q}_{i,o}\|) \times \Delta_{i,o}(\|\tilde{q}_i\|, \|\beta_i(\tilde{q}_i)\|, \|\dot{q}_i\|)\hat{r}_i$, $q_{i,o}$ denotes the position of the obstacle for the ith system, $\dot{q}_{i,o}$ is the relative velocity for the obstacle and the ith system, $I \in \mathbb{R}^{2n \times 2n}$ denotes the identity matrix. Additionally, $\mathcal{B}_{i,o} = \{q_i, q_{i,o} \in \mathbb{R}^2 : \|q_i - q_{i,o}\| \leqslant d_i\}$ marks a region $\rho_{i,or} = d_i$, where d_i is the minimum allowed safe distance between the ith system and an obstacle. $\rho_{i,o} = (\max\{\|q_i - q_{i,o}\|, d_i\} + d_i - \|\dot{q}_i - \dot{q}_{i,o}\|)$ is the mission function for obstacles avoidance. If the mission is active, $\tilde{\rho}_{i,o} = \rho_{i,or} - \rho_{i,o} \geqslant 0$, otherwise, $\tilde{\rho}_{i,o} = 0$, where $\tilde{\rho}_o = [\tilde{\rho}_{i,o}, \ldots, \tilde{\rho}_{i,o}]^{\rm T}$. Furthermore, $Q_{i,o} = \hat{r}_i^{\rm T}$ is the Jacobian matrix, $\hat{r}_i = (q_i - q_{i,o})/\|q_i - q_{i,o}\|$ is a unity vector pointing at the nearest obstacle, we denote $Q_o = [Q_{1,o}, \ldots, Q_{n,o}] \in \mathbb{R}^{1 \times pn}$. $\Delta_{i,o}(\|\tilde{q}_i\|, \|\beta_i(\tilde{q}_i)\|, \|\dot{q}_i\|) > 0$ is a state-dependent gain to be defined later, and $\dot{q}_\varsigma = [\dot{q}_{1,\varsigma}^{\rm T}, \ldots, \dot{q}_{n,\varsigma}^{\rm T}]^{\rm T} = Q_\varsigma^\dagger \Delta_\varsigma \tilde{\rho}_\varsigma$ is the desired velocity for the formation mission.

Theorem 2. Using the proposed control algorithm (6) and (7) with desired velocity (13) for system (1), the following results are hold.
Case 1: The generalized system errors $\tilde{q}_{i,j}$ and $\dot{\tilde{q}}_{i,j}$ will converge to $|\tilde{q}_{i,j}| \leqslant \eta_1$ and $|\dot{\tilde{q}}_{i,j}| \leqslant \eta_2$ in finite time if the motion and obstacle avoidance missions do not conflict, where
$\eta_1 = \max\{\epsilon, \min\{\frac{|o|}{c_1}, (\frac{|o|}{c_2})^{1/r}\}\}$ and $\eta_2 = |o| + c_1\eta_1 + c_2\eta_1^r$.
Case 2: If the obstacle avoidance mission is active and the overall missions are conflicting, the design parameter satisfies $\Delta_{i,o}(\|\tilde{q}_i\|, \|\beta_i(\tilde{q}_i)\|, \|\dot{q}_i\|) = \Delta_{i,o}^\star(\|\tilde{q}_i\|, \|\beta_i(\tilde{q}_i)\|, \|\dot{q}_i\|) + \varrho_i$, where ϱ_i is a robust term (e.g., rejection measurement noise). After finishing the obstacle mission, the motion mission continues. Moreover, the tracking errors $\tilde{q}_{i,j}$ and $\dot{\tilde{q}}_{i,j}$ will converge to η_1 and η_2, respectively, in finite time.

Proof. Similar to the proof of Theorem 1, Consider the overall Lyapunov function candidate V_2 as

$$V_2 = V_{\sigma 2} + V_{\rho 2}, \tag{14}$$

where $V_{\sigma 2}$ is considered to prove the stability of the systems under the proposed control laws, and $V_{\rho 2}$ is constructed to testify the stability of the missions including motion and obstacle avoidance.

First, $V_{\sigma 2} = V_{\sigma 1}$; therefore, the details are omitted here, as they are the same as the corresponding content of Theorem 1.

Second, the stability of the motion with obstacle avoidance should be proved. Define the Lyapunov function candidate $V_{\rho 2}$ for the motion mission as

$$V_{\rho 2} = \frac{1}{2}\gamma_o\tilde{\rho}_o^2 + \frac{1}{2}\tilde{\rho}_\varsigma^{\rm T}\gamma_\varsigma\tilde{\rho}_\varsigma, \tag{15}$$

where γ_o, γ_ς are positive constants, and $\tilde{\rho}_o = \sum_{i=1}^n \tilde{\rho}_{i,o}$. When the system moves without obstacles in its imminent surroundings, the item $Q_\varsigma Q_o^\dagger$ in (13) equals 0. Then we can obtain the derivative of V_ρ as

$$\dot{V}_{\rho 2} = -\gamma_o\tilde{\rho}_o \left[Q_o Q_o^\dagger \Delta_o\tilde{\rho}_o + Q_o(I - Q_o^\dagger Q_o)Q_\varsigma^\dagger \Delta_\varsigma\tilde{\rho}_\varsigma\right] - \tilde{\rho}_\varsigma^{\rm T}\gamma_\varsigma \left[Q_\varsigma Q_o^\dagger \Delta_o\tilde{\rho}_o + Q_\varsigma(I - Q_o^\dagger Q_o)Q_\varsigma^\dagger \Delta_\varsigma\tilde{\rho}_\varsigma\right]$$

$$= -\gamma_o \Delta_o \tilde{\rho}_o^2 - \tilde{\rho}_\varsigma^{\mathrm{T}} \gamma_\varsigma Q_\varsigma Q_\varsigma^\dagger \Delta_\varsigma \tilde{\rho}_\varsigma \leqslant 0. \tag{16}$$

From this, the formation (only the motion mission element) always maintains stable. Additionally, $\tilde{q}_{i,j}$ and $\dot{\tilde{q}}_{i,j}$ will converge to η_1 and η_2, respectively, in finite time. When there are obstacles in the nearby environments of the systems, the derivative of V_ρ is

$$\dot{V}_{\rho 2} \leqslant -\gamma_o \Delta_o \tilde{\rho}_o^2 - \tilde{\rho}_\varsigma^{\mathrm{T}} \gamma_\varsigma \left(Q_\varsigma Q_\varsigma^\dagger \Delta_\varsigma - Q_\varsigma Q_o^\dagger Q_o Q_\varsigma^\dagger \Delta_\varsigma \right) \tilde{\rho}_\varsigma + \frac{1}{2} \Delta_o \gamma_\varsigma Q_\varsigma Q_o^\dagger \left(\tilde{\rho}_o^2 + \|\tilde{\rho}_\varsigma\|^2 \right)$$

$$\leqslant -(\gamma_o - \frac{1}{2}\gamma_\varsigma \|Q_\varsigma\|) \Delta_o \tilde{\rho}_o^2 + \frac{1}{2} \Delta_o \gamma_\varsigma \|Q_\varsigma\| \|\tilde{\rho}_\varsigma\|^2, \tag{17}$$

where $\|Q_o\| = 1$ is used. The constraint $\gamma_o \geqslant \frac{1}{2}\gamma_\varsigma \|Q_\varsigma\|$ should be satisfied. In this situation, the system should end up tracking its desired trajectory for avoiding the obstacles. Redefine $V_{\rho 2}$ as $V_{\rho 2} = \frac{1}{2}\gamma_o \tilde{\rho}_o^2$, following (17) we have $\dot{V}_{\rho 2} = -\gamma_o \Delta_o \tilde{\rho}_o^2 \leqslant 0$. Furthermore, $\Delta_{i,o}$ should be designed properly to make the velocity error dominate the position error; this is necessary because the method used in this paper is a kinematic working on the dynamics through the desired velocity. We can calculate the largest value of $\Delta_{i,o}$ as

$$\Delta_{i,o}^\star(\|\tilde{q}_i\|, \|\beta_i(\tilde{q}_i)\|, \|\dot{q}_i\|) = \frac{-y_i + \sqrt{y_i^2 + 4x_i z_i}}{2x_i}, \tag{18}$$

where $x_i = \tilde{\rho}_{i,o}^2$, $y_i = -2\tilde{\rho}_{i,o}(\|\dot{q}_i\| + c_1\|\tilde{q}_i\| + c_2\|\beta_i(\tilde{q}_i)\|)$, $z_i = -\|\dot{q}_i\|^2 + c_1^2\|\tilde{q}_i\|^2 + c_2^2\|\beta_i(\tilde{q}_i)\|^2 + 2c_1\|\dot{q}_i\|\|\tilde{q}_i\| + 2c_2\|\dot{q}_i\|\|\beta_i(\tilde{q}_i)\| + 2c_1c_2\|\tilde{q}_i\|\|\beta_i(\tilde{q}_i)\|$ for $i = 1, \ldots, n$. Using the fact that $\varsigma_i^{\mathrm{T}} K_{si}\varsigma_i^s = k_{si}(\varsigma_i^{\mathrm{T}}\varsigma_i)^{\frac{s+1}{2}}$, Eq. (18) is also applied to the term $K_{si}\varsigma_i^s$ in the control law. We choose $\Delta_{i,o}(\|\tilde{q}_i\|, \|\beta_i(\tilde{q}_i)\|, \|\dot{q}_i\|) = \Delta_{i,o}^\star(\|\tilde{q}_i\|, \|\beta_i(\tilde{q}_i)\|, \|\dot{q}_i\|) + \varrho_i$, where $\varrho_i > 0$ is designed to show robustness to noise. This constraint ensures that the minimum related distances between system i and the obstacles are maintained at d_i.

Remark 1. It is worth mentioning that 'behavior' and 'mission' have the same meaning in this paper. Following such an NSB control architecture, very simple behaviors for each system are defined and property arranged in priority in order to achieve the overall assigned mission.

Remark 2. Utilizing the algorithms proposed in this paper, the convergence regions and time can be adjusted by tuning some related design parameters. Taking Theorem 2 as example, the discussion is similar with Lemma 3 of [35]. First, with the fixed convergence regions, the convergence time can be adjusted in the reaching phase by properly tuning the design parameters $c_{\sigma i}$, c_{si}, s, and the initial value of V_1 and, in the sliding phase, by properly tuning the design parameters, c_1, c_2, r, and the initial value of $\sigma_{i,j}$. For example, decreasing of s and r contributes to faster convergence and higher accuracy. Second, with a fixed convergence time, we can properly adjust the design parameter ϵ to minimize the regions. It is worth noting that the design parameters are coupling, thus how they act on the convergence regions and time might not be readily apparent. However, the relationship expressions regarding the convergence regions and parameters have been given accurately, so the change rules of some key parameters can be found by adjusting them while fixing all the other parameters. Then according to these expressions and rules, the design parameters can be adjusted properly to meet the specified performance indicators and control requirements.

4 Simulations

In this section, two simulation examples are proposed according to Theorems 1 and 2. Consider a five-node Euler-Lagrange system on a 2D plane. The five systems' parameters are assumed to be $M = [1; 1; 1; 1; 1]^{\mathrm{T}}$, $C = [0; 0; 0; 0; 0]^{\mathrm{T}}$. The formation control problem is to design control laws such that the five dynamics can form a formation in finite time with and without obstacle avoidance, respectively. And it assumes that the control torque $\|\tau_i\|_\infty \leqslant 20N$. The initial positions of the five systems are assumed to be $q_1 = [-16; 24], q_2 = [11; 12], q_3 = [39; -4], q_4 = [9; -16], q_5 = [-18; -31]$, and the desired formation mission functions for the five robots are: $\rho_{fd_1}[-14 + 2t; 28], \rho_{fd_2} = [14 + 2t; 14], \rho_{fd_3} = [42 + 2t; 0], \rho_{fd_4} =$

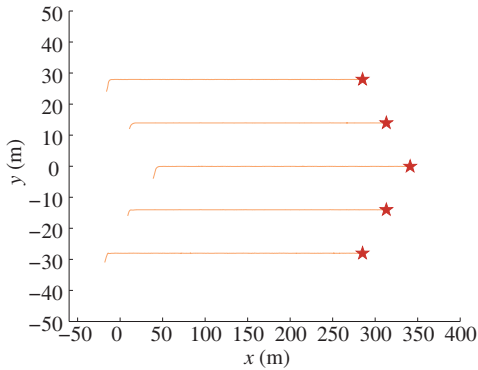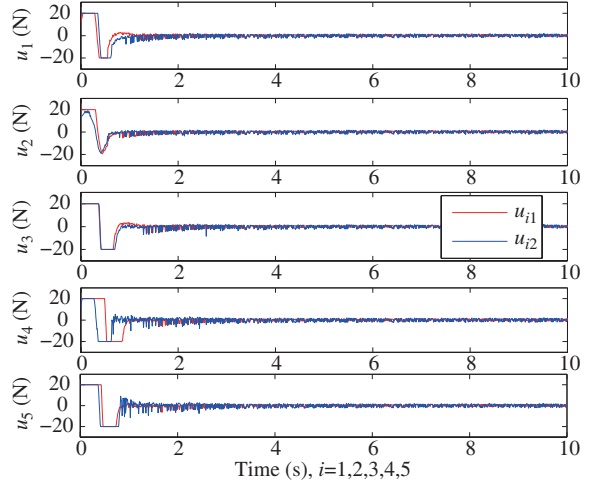**Figure 2** Trajectories of the formation without obstacles.

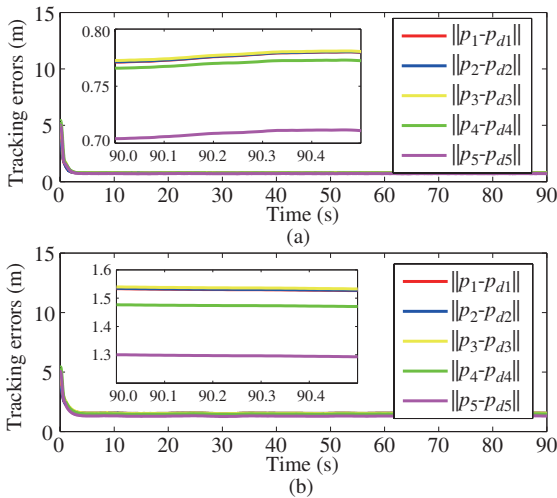**Figure 3** Response of the control force.

Figure 4 (a) Response of the tracking errors with finite-time convergence; (b) response of the tracking errors with asymptotic convergence.
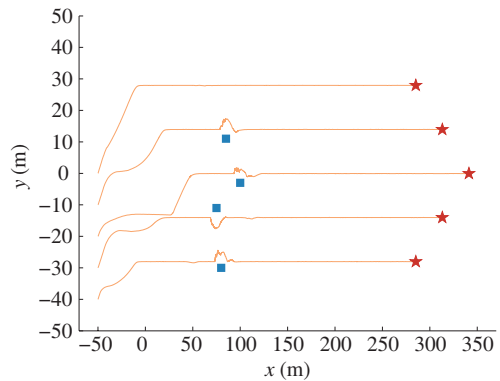

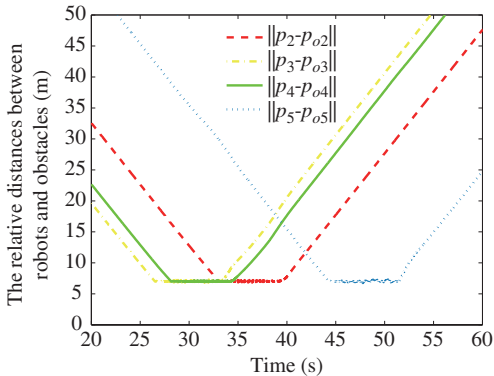**Figure 5** Trajectories of the formation with obstacle avoidance.

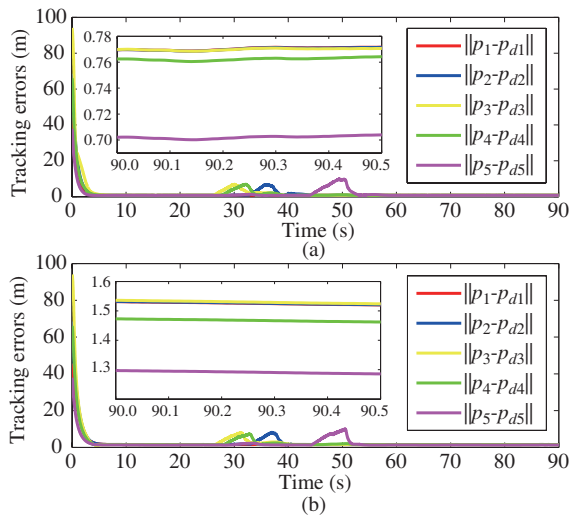**Figure 6** Relative distances between robots and obstacles.

Figure 7 (a) Response of the tracking errors with obstacle avoidance with finite-time convergence; (b) response of the tracking errors with asymptotic convergence.

$[14 + 2t; -14], \rho_{fd_5} = [-14 + 2t; -28]$, respectively. Figures 2–4 show the results of the five systems achieving a formation in finite time when there are no obstacles. The formation control problem can be solved with the aid of the results proposed in Theorem 1. Figure 2 shows the trajectories of the five systems, and the desired formation is clearly achieved in finite time. Figure 3 shows the corresponding control forces of the systems. Figure 4(a) shows the tracking errors with finite time convergence. As a comparison, a simulation example by using asymptotic controller is provided in Figure 4(b), which shows slower convergence speed and lower precision. Figures 2–4 demonstrate the effectiveness of Theorem 1.

Figures 5–7 demonstrate the effectiveness of Theorem 2. In this case, a platoon of robots is required to achieve a prescribed coordinate formation while avoiding obstacles. The initial positions of the five robots are assumed to be $q_1 = [-50; 0], q_2 = [-50; -10], q_3 = [-50; -20], q_4 = [-50; -30], q_5 = [-50; -40]$, and the obstacle positions are $O_2 = [85; 11], O_3 = [100; -3], O_4 = [75; -11], O_5 = [80; -30]$. The desired formation mission functions for the five systems are: $\rho_{fd_1}[-14 + 2t; 28], \rho_{fd_2} = [14 + 2t; 14], \rho_{fd_3} = [42 + 2t; 0], \rho_{fd_4} = [14 + 2t; -14], \rho_{fd_5} = [-14 + 2t; -28]$. Figure 5 shows the trajectories of the five systems and the desired formation is clearly achieved in finite time while avoiding obstacles. Figure 7 shows the relative distances between robots and obstacles. Figure 7 (a) and (b) present the comparison of the tracking errors in finite time and asymptotic convergence, respectively, which shows the superiority of the proposed algorithm.

5 Conclusion

In this paper, the coordination control problem of multiple Euler-Lagrange systems has been investigated for accurate formation in environments with obstacles by employing the NSB control architecture, N-FTSM control, and adaptive control mechanism. A novel controller was designed and utilized to achieve the overall formation architecture with fast convergence and high-precision while avoiding obstacles and guaranteeing the model uncertainty rejection objective. Finally, simulation examples demonstrate the effectiveness of the algorithm. Future work will focus on distributed finite-time coordination control of multi-agent systems with switching topologies.

Conflict of interest The authors declare that they have no conflict of interest.

References

1 Ren W, Beard R W. Distributed Consensus in Multi-vehicle Cooperative Control: Theory and Applications. London: Springer, 2008

2 Wang L, Jiang F C, Xie G M, et al. Controllability of multi-agent systems based on agreement protocols. Sci China Ser-F: Inf Sci, 2009, 52: 2074–2088

3 Wang Q, Wang Y Z. Cluster synchronization of a class of multi-agent systems with a bipartite graph topology. Sci China Inf Sci, 2014, 57: 012203

4 Min H, Wang S, Sun F, et al. Decentralized adaptive attitude synchronization of spacecraft formation. Syst Control Lett, 2012, 61: 238–246

5 Wang H. Flocking of networked uncertain Euler-Lagrange systems on directed graphs. Automatica, 2013, 49: 2774–2779

6 Mei J, Ren W, Chen J, et al. Distributed adaptive coordination for multiple Lagrangian systems under a directed graph without using neighbors' velocity information. Automatica, 2013, 49: 1723–1731

7 Nuño E, Ortega R, Jayawardhana B, et al. Coordination of multi-agent Euler-Lagrange systems via energy-shaping: networking improves robustness. Automatica, 2013, 49: 3065–3071

8 Chen F, Feng G, Liu L, et al. Distributed average tracking of networked Euler-Lagrange systems. IEEE Trans Autom Control, 2015, 60: 547–552

9 Meng Z, Ren W, You Z. Distributed finite-time attitude containment control for multiple rigid bodies. Automatica, 2010, 46: 2092–2099

10 Ren W. Distributed leaderless consensus algorithms for networked Euler-Lagrange systems. Int J Control, 2009, 82: 2137–2149

11 Sandell Jr N R, Varaiya P, Athans M, et al. Survey of decentralized control methods for large scale systems. IEEE Trans Autom Control, 1978, 23: 108–128

12 Balch T, Arkin R C. Behavior-based formation control for multirobot teams. IEEE Trans Robot Autom, 1998, 14: 926–939

13 Leonard N E, Fiorelli E. Virtual leaders, artificial potentials and coordinated control of groups. In: Proceedings of the 40th IEEE Conference on Decision and Control, Orlando, 2001. 2968–2973

14 Feddema J T, Lewis C, Schoenwald D. Decentralized control of cooperative robotic vehicles: theory and application. IEEE Trans Robot Autom, 2002, 18: 852–864

15 Belta C, Kumar V. Abstraction and control for groups of robots. IEEE Trans Robot, 2004, 20: 865–875

16 Olfati-Saber R, Fax A, Murray R M. Consensus and cooperation in networked multi-agent systems. Proc IEEE, 2007, 95: 215–233

17 Chung S J, Slotine J J E. Cooperative robot control and concurrent synchronization of Lagrangian systems. IEEE Trans Robot, 2009, 25: 686–700

18 Qu Z. Cooperative Control of Dynamical Systems: Applications to Autonomous Vehicles. London: Springer-Verlag, 2009

19 Arrichiello F. Coordination control of multiple mobile robots. Dissertation of Doctoral Degree. Cassino: Universita Degli Studi Di Cassino, 2006

20 Antonelli G, Chiaverini S. Kinematic control of platoons of autonomous vehicles. IEEE Trans Robot, 2006, 22: 1285–1292

21 Antonelli G, Arrichiello F, Chiaverini S. The null-space-based behavioral control for autonomous robotic systems. Intell Serv Robot, 2008, 1: 27–39

22 Marino A, Parker L E, Antonelli G, et al. A decentralized architecture for multi-robot systems based on the null-space-behavioral control with application to multi-robot border patrolling. J Intell Robot Syst, 2013, 71: 423–444

23 Huang J, Fang H, Dou L, et al. An overview of distributed high-order multi-agent coordination. IEEE/CAA J Automat Sin, 2014, 1: 1–9

24 Cheng L, Hou Z G, Tan M. Decentralized adaptive consensus control for multi-manipulator system with uncertain dynamics. In: Proceedings of IEEE International Conference on Systems, Man and Cybernetics, Singapore, 2008. 2712–2717

25 Cheng L, Hou Z G, Tan M. Decentralized adaptive leader-follower control of multi-manipulator system with uncertain dynamics. In: Proceedings of 34th Annual Conference of IEEE In Industrial Electronics, Orlando, 2008. 1608–1613

26 Dong W, Farrell J. Cooperative control of multiple nonholonomic mobile agents. IEEE Trans Autom Control, 2008, 53: 1434–1448

27 Yang Q, Fang H, Mao Y, et al. Distributed tracking for networked Euler-Lagrange systems without velocity measurements. J Syst Eng Electron, 2014, 25: 671–680

28 Stilwell D J, Bishop B E. Platoons of underwater vehicles. IEEE Control Syst Mag, 2000, 20: 45–52

29 Olfati-Saber R, Murray R M. Distributed cooperative control of multiple vehicle formations using structural potential functions. In: Proceedings of the 15th IFAC World Congress, Barcelona, 2002. 346–352

30 Wang X, Yadav V, Balakrishnan S N. Cooperative UAV formation flying with obstacle/collision avoidance. IEEE Trans Control Syst Technol, 2007, 15: 672–679

31 Hou Z G, Cheng L, Tan M. Decentralized robust adaptive control for the multiagent system consensus problem using neural networks. IEEE Trans Syst Man Cybern Part B-Cybern, 2009, 39: 636–647

32 Cheng L, Hou Z G, Tan M, et al. Neural-network-based adaptive leader-following control for multiagent systems with uncertainties. IEEE Trans Neural Netw, 2010, 21: 1351–1358

33 Zhou N, Xia Y, Lu K, et al. Decentralised finite-time attitude synchronisation and tracking control for rigid spacecraft. Int J Syst Sci, 2015, 46: 2493–2509

34 Zhou N, Xia Y, Wang M, et al. Finite-time attitude control of multiple rigid spacecraft using terminal sliding mode. Int J Robust Nonlinear Control, 2015, 25: 1862–1876

35 Zhou N, Xia Y. Coordination control design for formation reconfiguration of multiple spacecraft. IET Contr Theory Appl, 2015, 9: 2222–2231

36 Yu S, Yu X, Shirinzadeh B, et al. Continuous finite-time control for robotic manipulators with terminal sliding mode. Automatica, 2005, 41: 1957–1964

37 Kwon J W, Chwa D. Hierarchical formation control based on a vector field method for wheeled mobile robots. IEEE

Trans Robot, 2012, 28: 1335–1345

38 Ranjbar-Sahraei B, Shabaninia F, Nemati A, et al. A novel robust decentralized adaptive fuzzy control for swarm formation of multiagent systems. IEEE Trans Ind Electron, 2012, 59: 3124–3134

39 Kan Z, Dani A P, Shea J M, et al. Network connectivity preserving formation stabilization and obstacle avoidance via a decentralized controller. IEEE Trans Autom Control, 2012, 57: 1827–1832

40 Fukushima H, Kon K, Matsuno F. Model predictive formation control using branch-and-bound compatible with collision avoidance problems. IEEE Trans Robot, 2013, 29: 1308–1317

41 Oh K K, Ahn H S. Formation control and network localization via orientation alignment. IEEE Trans Autom Control, 2014, 59: 540–545